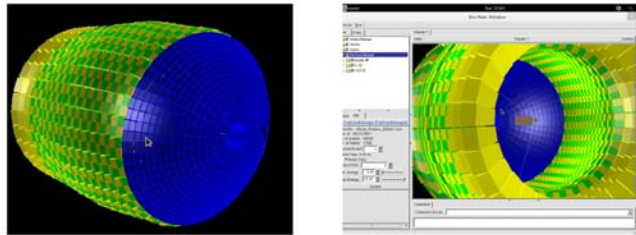


The R3B meeting <http://161.111.23.177/r3bmeeting/> held in Madrid (10-14 December 2012) offered a great amount of novel ideas. Several different subjects were discussed, like: Advances in APDs, Scintillator materials, silicon photomultipliers, analytical methods to study the signal response, advance in n-gamma separations and particle identification in homogeneous scintillators, hardware implementation and experimental tests of PSA codes for the relevant Phoswich detectors, improvements in DAQ and signal processing, simulation of light transport inside large volume detectors, develop of more efficient hit position finder algorithms, design of large volume scintillator and hybrid detector demonstrator like the end cap CEPA of CALIFA, experimental tests in different facilities like GSI to test scintillator detectors with gamma radiation and protons of high energy, tests of Phoswich detectors of LAbE+LaCl or LaBr + NaI crystal arrays, simulation of gamma cascades and reaction (p, 2p) with large volume and hybrid detectors, etc. and allowed for discussions and to take advantage of the expertise of each institute in a coordinated way.

R³B **Status of Phoswich Endcap Design and Simulations CEPA-10**



*J. Sánchez del Río, E. Nácher, A. Perea and O. tengblad
R3B Meeting, Madrid, Dec. 2012
IEM-CSIC MADRID*



Fig 2. Status of CEPA CALIFA endcap design and simulations presented at R3BMeeting held in Madrid, Dec, 2012 <http://161.111.23.177/r3bmeeting/>

Results have been presented at other schools and meetings, like the International Scientific Meeting on Nuclear Physics held in La Rábida, Huelva, Spain (9th-13th sept. 2013) or the EFN2012 in the same place (14-16 Sept. 2013), which have contributed to disseminate to the broader scientific community some of actual advances in nuclear physics topics that are related to GANAS, more specially topics based on time response of the CeBr3 crystals, non proportionally study in single crystals scintillators and the Phoswich scintillator for gamma and proton detection.

The next collaboration meeting will be held 4th of July 2013 at IFJ PAN Krakow.

Work package 1. New Materials **General background**

Detection properties of new advanced scintillator materials like CeBr_3 crystals or phoswich $\text{LaBr}_3\text{-CsI}$ phoswich scintillators or SrI_2 have been studied for their use in a gamma spectrometer.

The ideal inorganic scintillator should provide not only a high light yield but also a high effective atomic number for good stopping power, a short decay time constant for fast response, and a good level of linear response for good energy resolution. In addition, chemical and mechanical robustness are needed to allow the scintillator detector to be used in many different applications and environments.

The main objectives of this work package (WP1) are the study of the detection properties of new advanced scintillator materials and to assess the performances for its use in a gamma spectrometer.

With the idea of reducing some costs, CeBr_3 crystals have been studied. They have very similar properties to LaBr_3 and LaCl_3 crystals, though they are not as efficient. Its lower cost (approx. price: 10 €/cm³), good time and energy resolution and its absence of intrinsic radioactivity make them good candidates to be used as scintillator crystals for high volume detectors.

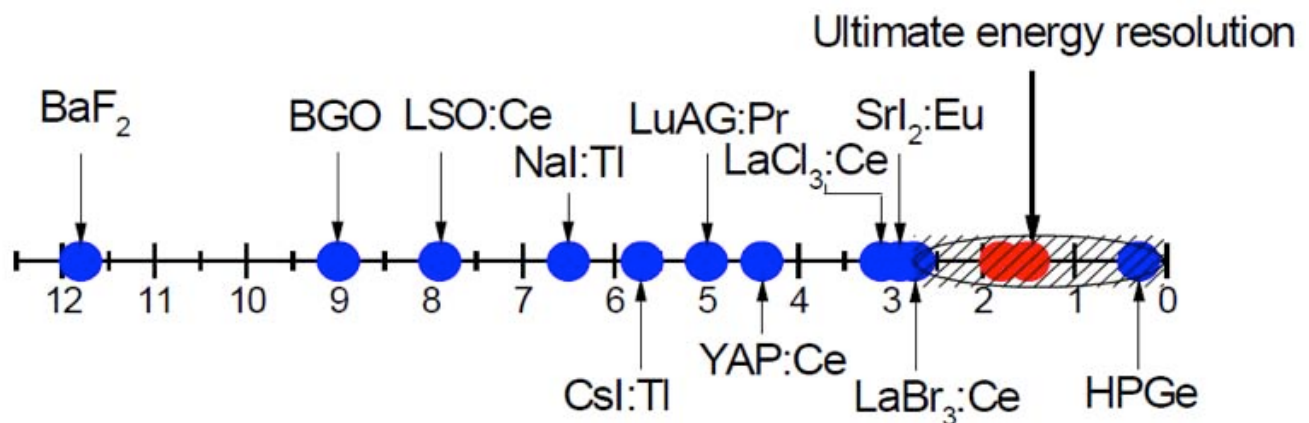


Fig 1. Existing High resolution scintillators: FWHM in % at 662 KeV.

A field of interest for the proposed study will concern scintillating transparent ceramics. This means the study of different solutions for the proper encapsulation and packaging of the crystals as well as in the optical coupling with the most suited photo detector. The encapsulation usually requires external pressure for the crystal and this property is

highly connected with non proportionality, that seriously affects to the optical response. It depends on the crystals structure, dopant concentration, concentration in caption substituted materials and crystals structure.

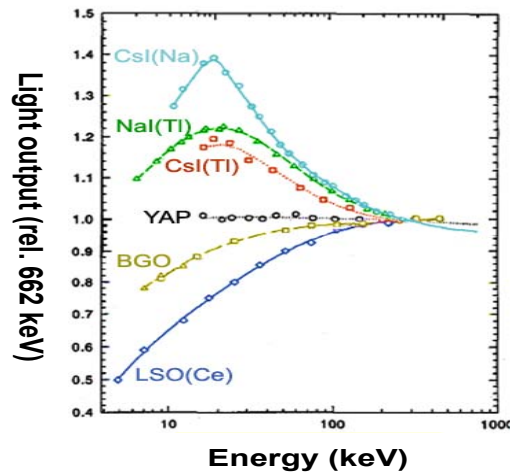


Fig 2. Light output vs Energy for some typical scintillators.

The ideal inorganic scintillator should provide not only a high light yield but also a high effective atomic number for good stopping power, a short decay time constant for fast response, and a good level of linear response for good energy resolution. To all these properties, chemical and mechanical robustness would be as well recommendable for the deployment of the scintillator detector in many application and different environments.

Summing up, in the latest year there is therefore a renewed interest, in the chemistry and material science community, to search for new luminescent inorganic crystals as real alternatives to $\text{LaBr}_3:\text{Ce}$. While many of the new proposed scintillators are still in the developing process and are not available in sizes suitable for our interest, there are few, as CeBr_3 or $\text{SrI}_2:\text{Eu}$, that have already been grown in cm^3 scale samples. In particular, CeBr_3 provides a light yield of 68 photons/keV and a fast decay time and $\text{SrI}_2:\text{Eu}$, while being brighter with a light yield close to 100 photon/keV, has a long decay time constant (around 1 μs) and a very linear response.

Work package 1. New Materials 2012 progress report

The main objectives of this work package are the study of the detection properties of new advanced scintillator materials and to assess the performances for their use in gamma spectroscopy for nuclear physics.

It is furthermore our interest to create a network with expert laboratories and companies that produces these new promising scintillator materials.

Detector's procurements

IPNO received for the GANAS project 39000 € over the first two years. This money has been asked to procure new advanced scintillator crystals and photomultipliers tubes to test them.

Crystal	Geometry	Manufacture	Price	Delivery
CeBr3	Ø 25 mm x 25 mm	Scionix	1,475€	In 2011
CeBr3	Ø 51 mm x 76 mm	Scionix	15,200€	November 2012
SrI2:Eu	Ø 25 mm x 25 mm	RMD	12,600\$(9420€)	Expected March 2013
CLYC	Ø 25 mm x 25 mm	RMD	7,000\$(5701€)	Expected March 2013

PMT	Features	Manufacture	Price	Delivery
5 R7723-100	Ø 51 mm – SBA photocathode 8 dynodes	Hamamatsu	478.80€ (2,394€ total)	January 2013

Milano has bought a 1"x1" CLYC crystal from RMD manufacturer. The detector arrived in December 2012. Milano has also several LaBr3:Ce detector of different sizes, from 1"x1" up to 3.5" x 8". All these detectors were NOT bought with GANAS funds.

Scintillator characterizations

The two CeBr3 crystals have been fully characterized with gamma ray emitting sources in the energy range between 60 to 1408 keV. In particular we measured the light yield, the energy resolution, the gamma ray proportionality and, for the 76 mm thick CeBr3, the light yield uniformity.

The tests have been performed coupling the crystals to a PMT Hamamatsu R7723-100, equipped with a Ø 51 mm entrance window and a super-bialkali photocathode. The gamma ray spectra have been acquired with a standard spectroscopic chain: the anode signal from the phototube was sent to a cremat 113 preamplifier, then shaped with an ORTEC spectroscopy amplifier and finally collected with an ADC. For the two CeBr3 crystals we measured an energy resolution at 662 keV of 4.8% and 4.7% for the small and the big volume crystal respectively.

In Milano the large volume LaBr3:Ce detectors have been fully characterized. We tested the detectors using monochromatic gamma-ray sources and in-beam reactions producing gamma-rays up to 22.6 MeV. We acquired PMT signal pulses and calculated detector energy resolution and linearity of response as a function of gamma-ray energy. Two different voltage dividers were coupled to the PMT: the Hamamatsu E1198-26, based on straightforward resistive network design and the "LABRVD", specifically designed for our large volume LaBr3:Ce scintillation detectors, which also includes active semiconductor devices. We also estimated the time resolution of different sized detectors (from 1"x1" up to 3.5"x8"), correlating the results with the intrinsic properties of PMTs and the GEANT simulations of the scintillation light collection process. A NIM paper is going to be submitted.

Concerning the measurements with the 1"x1" CLYC scintillator in Milano, the measurements are still in progress. We plan to compare the scintillator response using different PMTs, voltage dividers, and values of HV. We will measure energy resolution with different shaping times, preamplifiers and for

different gamma rays energies. In addition, we plan to measure the neutron response using PSA digital technique and the specific modules we have designed for BaF2 and LaBr3:Ce.

In beam test at ALTO (May 2013)

The five scintillators procured within the frame of the GANAS collaboration will be tested in May 2013 during an in beam testing of clusters for the PARIS demonstrator. This campaign will lead us to test the scintillators at gamma ray energies not available with standard radioactive sources. Each scintillator will be coupled to a R7723-100 photomultiplier tube from Hamamatsu, as used for the phoswich light readout by the PARIS collaboration, and the signals will be collected by a 1 GS digitizer for offline analysis.

WORKING-PACKAGE 2

EVALUATION OF NEW IMPROVED VERSIONS OF TWO 100 MM² APDs PACKAGED IN A COMMON FRAME (HAMAMATSU) (USC)

EVALUATION OF A PROTOTYPE SYSTEM OF SILICON PHOTOMULTIPLIERS COUPLED TO LABR IN A MAGNET (YORK)

Pankaj Joshi, David Jenkins, Nuray Yavuzkanat

Department of Physics, University of York, York YO10 5DD, United Kingdom

Large area silicon avalanche photodiodes (APD) when used with different scintillators can be an excellent soft gamma-ray detector. In particular, so called reverse type APD is well suited for these applications due to very narrow, no more than 8 mm thick, high gain layer close to the light entry surface and optimized for high efficiency detection of short wavelength radiation. The special gain profile of the structure provides amplification where it is needed and does not introduce additional noise in the rest of the structure, which has a wide depletion region necessary to minimize device capacitance. Low device capacitance is important parameter from the point of low noise operation requirements when connected to interface electronics, but in this case is aggravated by device very large size and only through this special design it has been possible to achieve acceptable capacitance while keeping breakdown at reasonably low level at the same time.

Currently there is only one producer on the market that provides a detector series fulfilling all the requirements in a device large enough to be used in large volume scintillation detectors. The Hamamatsu series S8664 shows up with a type leakage current of 10 nA at gain of 50 and a terminal capacitance of 270pF for their largest device of 100 mm². There is some development going on in this company to change the shape of this device e.g. for the panda experiment, but currently not so much effort is put into the development of even larger size sensors. Recent investigations have shown that increasing the active area from 1 cm² to 2 cm² significantly improves the performance of a scintillation detector [USC paper].

Collaboration partner *Technische Universität München* in collaboration Laser Components DG, Inc. have started a new development is to produce fully functional 10 x 20 mm active area detectors, which shape and size is not commercially available at the moment. This project co funded by the BMBF is focused on fully functional prototypes mounted on a ceramic subcarrier with device completely immersed in clear plastic coating.

This detectors have to be directly compared to the Hamamatsu standard for a different applications to specify all parameters essential for spectroscopic light detection like e.g. temperature dependence,

spectral response, signal rise time gain curves stability radiation hardness. Having a second producer on the market will strongly influence the further developments as well as the price policy of the companies and by this influence all the projects discussed here.

The company NUVIA is interested in some of this technology to use in nuclear industry. The idea is turn some of this work in to a commercial company with a second company.

In this package APDs have been evaluated in conjunction with the LaBr₃ scintillators. Energy resolutions of 6-7 % and timing resolutions of 1-2 ns were measured. SiPMs. have been studied and compared with APDs as well. APDs can be used for nuclear physics studies and wider applications in medical imaging and elsewhere. The insensitivity of the prototype systems to magnetic field has been verified.

Scintillation detectors are important for charged-particle and gamma-ray detection both in nuclear physics, and medical and industrial applications. Conventionally, the best performance in terms of scintillation light collection is obtained with photomultiplier tubes (PMTs). Such PMTs cannot be operated in regions of high magnetic field. This imposes a strong restriction on the efficient employment of scintillator detectors in high magnetic field environments commonly found in various apparatus of interest in nuclear physics. In addition, there is very strong interest in the medical sector in combined imaging where it is desirable to perform positron-emission tomography (PET) or single-photon emission computed tomography (SPECT), which provide functional information, simultaneously with MRI, which provides anatomical information. This means that the scintillator-based technologies associated with PET or SPECT would need to be operated within the high magnetic field of an MRI magnet. It turns out that this need from the medical side aligns very well with topical interests in nuclear physics, where gamma ray detection is required in high magnetic field environments. Imaging systems, however, have two additional constraints. One is that RF-induced noise may affect the performance of the PET system. The second is the magnetic field is more susceptible to the placement of external objects (i.e. sensors and detectors).

A prototype gamma-ray detector systems which could be used in high magnetic field environments has been evaluated. A specific project of interest is a gamma-ray detector array to be used in conjunction with a helical-orbit spectrometer such as the HELIOS spectrometer at Argonne National Laboratory [Lig10,Wuo07]. Such a spectrometer is intended to study single-particle transfer reactions in inverse kinematics. The spectrometer comprises a large solenoidal magnet (such as a redundant MRI magnet) in which light ions from the reaction follow helical orbits before being detected along the axis in a compact linear silicon array. Detection of gamma rays would assist in assigning j values to observed states and in other applications. In this case, the gamma ray array would need to have high energy resolution but be capable of operating in a magnetic field up to 3T. With the intention of achieving the highest possible energy resolution we considered the new generation scintillator material, lanthanum bromide, which has an intrinsic resolution better than 3% for 662-keV gamma rays. For the scintillation light collection, we focused mainly on APDs since they have low noise and good temperature stability. However, SiPMs (which are arrays of APDs working in Geiger mode) were also studied for the sake of completeness. Survey of available sensors: The principal manufacturer of APDs is Hamamatsu. Although we used mostly Hamamatsu APDs and SiPMs for this work, it is worth mentioning that there are few other companies which make such sensors including SensL (Ireland) and Photonique SA (now available from Advatech-UK). Photonique's sensors originate from CPTA Russia. These were not particularly useful to us as their efficiency in lower wavelength (380 nm) was negligible. Some measurements were also made using SiPMs from Hamamatsu – models 10362-11-025U and 10363-33-

025C which were 1mm x 1mm and 3mm x 3mm in size. The 1 mm device was not useful for making an energy measurement due to its small size and thus small light collection efficiency, but it was possible for it to be used as trigger for timing. We also tested some of SensL's earlier devices like their 4 x 4 array (or tile) but their efficiency was again not anywhere close to being suitable for use with LaBr₃(Ce). These devices may, however, be used in imaging applications where the scintillation photons are longer wavelength (500-600 nm). We have future plans to build a small imaging system using 4 x 4 two dimensional arrays where we plan to do a comparison between the Hamamatsu and SensL device (4 x 4 tile) which are both sensitive to the higher wavelength region where emission takes place in LYSO and BGO. Description of work carried out: The simple prototype which was the main goal of the study was constructed from a Hamamatsu APD with an LaBr₃(Ce) scintillator as shown in the picture. The APDs used were S8664-1010 and S8664-55 devices from Hamamatsu which had dimensions of 10mm x 10mm and 5mm x 5mm, respectively. The LaBr₃(Ce) crystals are from St Gobain and are in a cylinder of 1cm diameter and 1 cm depth encased in an aluminium canister. The APDs were mounted on a small PCB (see fig. 6) with a non magnetic SMC connector on the back. Since the scintillator face was 10 mm, which was close to both the sensor dimensions, no light guides were used. The mounting of the APD on the scintillator was done using EJ-550 silicone gel obtained from ELJEN technologies and the sensor/detector system was wrapped in several layers of Teflon tape. Finally, they were wrapped in Al foil and then black masking tape to make them light-tight. The whole assembly was less than 1 cubic inch and connected to the preamplifier by a single cable. Mesytec unit MSI-8p was used as the preamplifier along with an Ortec 572 shaping amplifier for shaping and amplification. Power to the sensors was provided using Mesytec's MHV4 unit. Figures 7 and 8 show the performance of the sensor/scintillator system using ⁶⁰Co and ¹³⁷Cs sources, respectively.



Figure 6. LaBr₃ detector and the 5x5 mm and the 10x10 mm APD sensors used for measurements

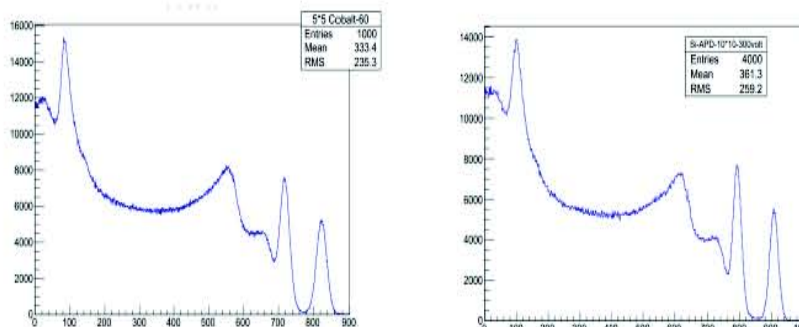


Figure 7. ⁶⁰Co spectra using a 5 x 5 mm and a 10 x 10 mm APD with LaBr₃(Ce) scintillator with energy resolution of 4.23 % and 3.57 % at 1332-keV

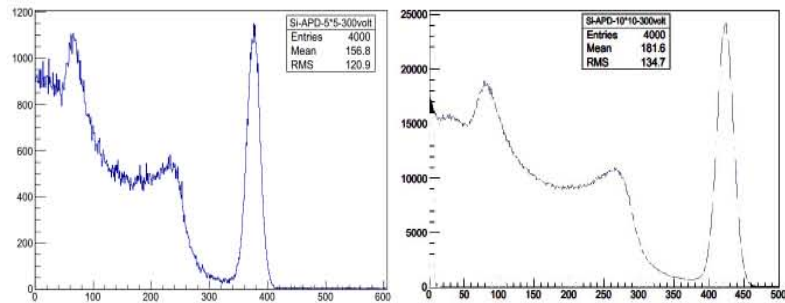


Figure 8. ^{137}Cs spectra using 5 x 5 mm and 10 x 10 mm APD with $\text{LaBr}_3(\text{Ce})$ scintillator with energy resolutions of 7.3 % and 6.7 %, respectively, at 662 keV

Magnetic field measurements: The performance of the prototype systems in a magnetic field was evaluated using a 1T magnet available in the Department of Physics at the University of York. The magnet belongs to the magnetic materials group and is a simple DC current magnet with sufficient in-pole gap to place the detector and APD. The preamplifier and the counting system remained on a trolley nearby. A ^{137}Cs source was used for the experiment and the measurements were done in the same setting with and without the 1-T magnetic field. The effect of the magnetic field on the performance of the detection system was found to be negligible. These measurements were then repeated by changing the orientation of the detector with respect to the magnetic field placing the detector axis perpendicular as well as parallel to the field axis. None of these measurements showed any deterioration in the performance in the magnetic field therefore suggesting that such a device would not be affected by the magnetic fields typically found in MRI magnets.



Figure 9. The 1T Magnet, used for the study. The detector set-up can be seen in between the pole pieces in the bottom right figure.

Although APDs were the main focus of the tests, it was found that SiPMs showed similar insensitivity to magnetic field, which is not so surprising given they are 2D array of tiny APDs and therefore, supposed to have similar characteristics. There was still the question of whether the insertion of the sensor and scintillator would modify the magnetic field or not. In order to investigate this aspect, we decided to perform an MRI scan of a phantom with the detector unit placed next to the phantom. The scan was performed at the York Neuroimaging Center (YNIC). Due to a restriction imposed by YNIC,

it was not possible to place measuring instruments (NIM bin, preamp etc.) inside the room containing the MRI machine. It was also not possible to use radiation sources within the facility. However, it was still possible to place the detector and the cables unit within the magnet's center alongside a phantom (a plastic ball filled with paramagnetic substance + H₂O) and perform a scan to see if any distortion to the image occurs. We used a 10 x 10 mm APD mounted on a 2.5 cm x 2.5 cm CsI(Tl) crystal and 5 x 5 mm APD mounted to an LaBr₃(Ce) encapsulated in aluminum. The connectors had 5 m long RG58 shielded cables connected with them. The images acquired by scanning this system showed that there was a small influence on the magnetic-field homogeneity from the detector set-up when it was placed alongside the phantom which was placed close to the axis of the magnet. The distortion caused to the image was small and it was possible to correct it using the shimming coils available in the MRI system. Placing the detection set-up far away from the axis, where most likely it would be used in a research set-up like HELIOS or in an imaging scanner (PET insert for an MRI scanner), did not show any image distortion of the scanned object.

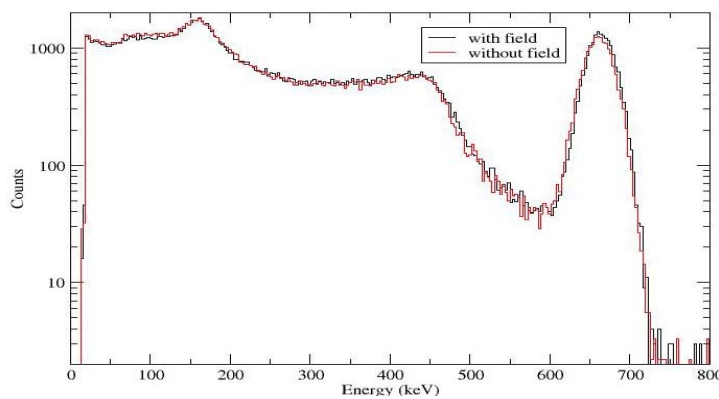


Figure 10. A representative set of spectra for a ¹³⁷Cs source obtained with and without 1T magnetic fields



Figure 11. The 3T MRI magnet at the York Neuroimaging Centre. The detectors are placed on the side of circular cage shown in the centre of the magnet. The cables from the detectors can be seen stretching along the bed

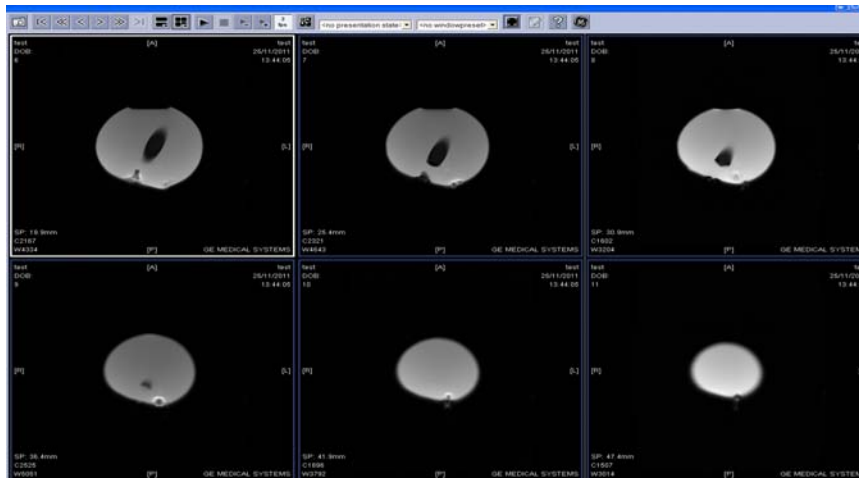


Figure 12. The MRI scan shows various cross sectional images of a phantom, taken at several depths along the magnetic field axis. The distortion of the magnetic field due to the detectors is apparent from the distortion in the images. This distortion can easily be corrected by shim coils in an MRI system. In normal use, the detectors will generally lie much further out and would cause minimal distortion to the field.

Timing measurements: Timing measurements were also performed using APDs. Since the timing of $\text{LaBr}_3(\text{Ce})$ is $\ll 1\text{ns}$, almost all of the timing resolution is contributed by the APD sensors and the electronics. The setup used for the timing is as shown in the figure 8. Using this circuit, TAC spectra for a coincidence between the two APD+ $\text{LaBr}_3(\text{Ce})$ were obtained. The timing resolution for the APD was found to be about 1.6 ns (see fig 13). We also realized the need to study timing spectra using an SiPM as these could be potentially useful device in the PET systems where energy resolution is not of very prime importance. For the SiPM, a TAC was generated using SiPM+ $\text{LaBr}_3(\text{Ce})$ in coincidence with a BaF_3 +Photomultiplier. A timing resolution of 2.2 ns was obtained (see fig 14) for this.

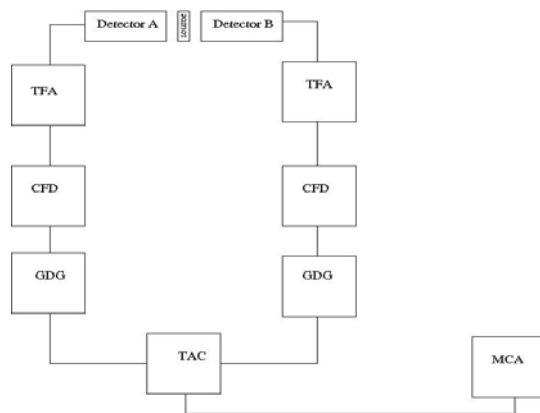


Fig 13: A general schematic representation of the set-up used for timing studies. The source used was ^{22}Na generating two gamma rays of 511 keV emitted near back-to-back.

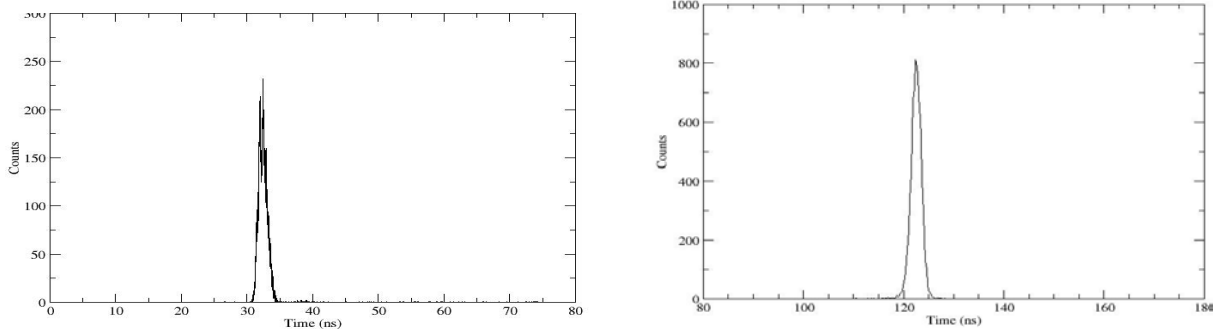


Fig 14: (left) TAC spectrum from coincidence between two Hamamatsu APDs (S8664). One of them was 5 x 5 mm while the other was 10 x 10 mm. A timing resolution of 1.6 ns was obtained. (right) TAC spectrum from coincidence between a SiPM + LaBr3, and BaF2 + photomultiplier. A timing resolution of 2.2 ns was obtained.

SiPM used low energy background reduction: As stated earlier, SiPMs were the less favorable devices for study as their use in spectroscopic energy measurement is limited by the problems like the higher levels of dark current related noise and temperature instability. Non spectroscopic applications like PET/SPECT systems are possible places where these could still be used effectively. There are indeed ways to overcome the problems to some extent. The temperature can be reduced and made more stable using Peltier-cooled devices which are the new version of devices being made available now by Hamamatsu. Another possible way to reduce the effect of the noise related background in the SiPM is to read the light output from a given event using two light sensors. A coincidence between the two would occur when a genuine event (interaction) would generate scintillation light in the detector. In the case of noise the signal from one of the sensors would generally not show a coincidence with the signal from the other sensor. Thus the coincidence technique would be able to clean up the lower energy background.

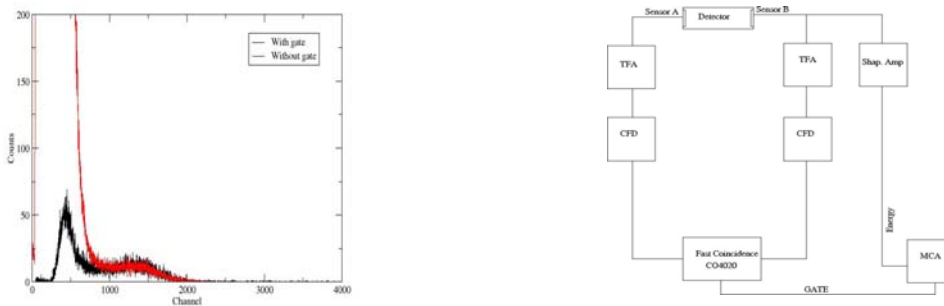


Fig 15:(on the left) energy spectrum from ^{137}Cs source using a 1 “ x 1 “ face CsI(Tl) with 3x3 mm SiPM sensor (shown in red) and the same (in black) when in coincidence with another sensor of 1x1 mm was demanded. This is to demonstrate that coincidence with another sensor helps in removing the lower energy noise. The schematic of the circuit used is shown on the right hand side.

The effectiveness of this technique could decrease with increasing voltage on the sensors as more and more random coincidences would then start appearing within the coincidence window due to larger amount of dark current. We did a preliminary investigation to test this. Although LaBr3(Ce) was a good candidate scintillator to test such a technique but it was not possible to put the two sensors

together on the small size crystal we had. Consequently we tried this technique using CsI(Tl) crystal which has two 1 inch faces available. Figure 15 shows the schematic of the set-up used and the spectra obtained using with and without coincidence gates. Hamamatsu 10362-11-025U (1x1 mm) and 10362-33-025C (3x3 mm) SiPM devices were used for this measurement. The result showed significant improvement in the background for lower energies. One would need more rigorous tests with various scintillators and sensor combinations as well as tests with various bias voltages in order to establish it as a useful technique. Conclusions: The following discussion describes our general conclusions about the two available possibilities: APD-based set-up: We aimed to build a simple prototype unit which could be used for spectroscopic energy and timing measurement in physics experiments. The use of APD in place of photomultiplier would allow for such a device to be used in high magnetic field. The device built using an APD and LaBr₃(Ce) fulfilled the minimum requirements for such a system. The energy resolution of 6-7 % and timing resolution of 1-2 ns would allow discrete gamma-decay studies to be carried out in coincidence with a charged particle detection set-ups like HELIOS without being affected by the magnetic field. SiPM-based set-up: This work also allow us to gain understanding which is applicable in a variety of applications of APD as well as SiPM. SiPM have less energy resolution compared to the APD. The energy resolution requirements of a PET imaging system are less stringent than those for spectroscopy work, therefore, a setup built using the prototype unit of APD would obviously work in scanning system. However, one of the main issues in the PET insert MRI is the high noise arising due to high-power RF and thus the best solution is to use electronics components close to the sensors. Customized ASICs could be the answer to such a problem. On the basis of this short discussion we feel SiPM can replace the APD both in the spectroscopic as well as the imaging applications only if their major pitfalls are taken care of. For the imaging application, one would need customized ASIC-based electronics, which is close to the sensors. In research applications leading to spectroscopy this is not a problem but the inherent noise needs to be removed to gain sufficient energy resolution from the SiPM. This can be achieved by using Peltier cooled SiPM combined with a coincidence gating technique mentioned earlier. Therefore the use of SiPM in both research and industrial applications would need to be carefully considered and optimised. Once used in this way, SiPM could be excellent devices as they have sufficient efficiency for the lower wavelength scintillation (see fig 16).

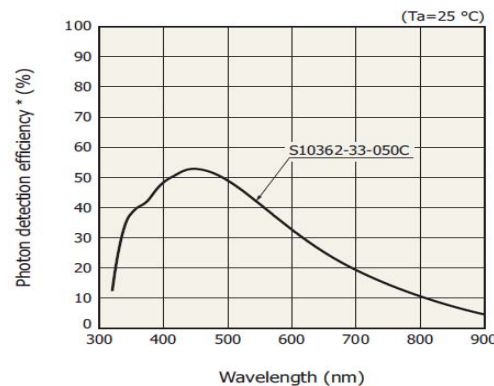


Fig 16: A plot of photon detection efficiency of Hamamatsu SIPM (S10362 series). At 380 nm it has an efficiency of 40%-50%.

References:

- [Lig10] J.C. Lighthall et al., NIM A 622, 97 (2010).
- [Wuo07] A.H. Wuosmaa et al., NIM A 580, 1290 (2007)

WORKING PACKAGE 3 (WP3)

Optimized PSA of the LaBr+LaCl crystal response from millstone 5.1 truncated pyramid.

In the experiment S404 held in GSI, 10^5 deuterons/s in a 5 mm target of CH₂ were launched at the energies: 200, 400, 600, 800, 1050 and 1500 MeV to test the different detectors of the R3B set-up. GANAS participated as “parasites” on the beam time placing our Scintillators in the way of the emitted protons:

1. IEM-CSIC-MADRID: an array CEPA4 consisting of 2x2 LaBr-LaCl crystals of 4+6 cm depth and a side base of 2.7 cm/crystal.
2. TU Munich: 2 phoswich crystals of LaBr+NaI and 2 crystals of NaI.
3. USC an array of 25 CsI crystals of the CALIFA barrel prototypes
4. CTH 1 CsI crystal from the crystal ball detector with silicon detectors to test possibility to use cosmic rays for proton energy calibration.

E_d AMeV	Beta	angle d deg.	angle p deg.
200	0.5677	30.5	--
400	0.7145	20.3	43.5
600	0.7938	15.8	33.1
800	0.8430	13.2	27.2
1050	0.8826	11.0	22.6
1500	0.9237	8.6	17.5

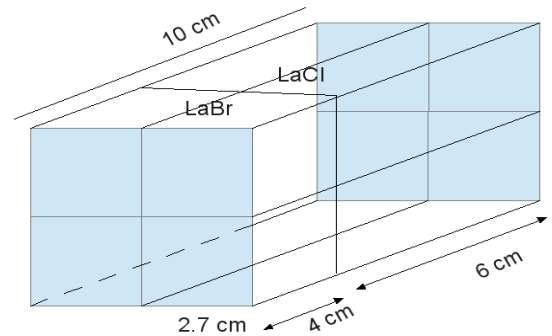


Fig 17: Energy of the deuteron primary beam

Fig 17: CEPA4 geometry design

We have studied the shape of the signal obtained for protons of different energies interacting with the array of scintillator crystals. Some simulations have been done before to compare them with real data plots. We can identify the protons of different energies representing the fast component of the signal vs the slow component. Data being analysed

**Working package 4:
Evaluation of optimal light read-out to gain 3D position resolution (Giessen)**

**Simulation of scintillator light transport inside light volume detectors (Milano)(12 months)
and
Development of an algorithm for hit position identifications (24 months)**

Alpha-Gamma discrimination by Pulse Shape in LaBr₃:Ce and LaCl₃:Ce

WP4. Position Sensitivity in Large Crystals & Applications

This research program addresses the development of technology needed to localize the interaction points of gamma-rays inside a large volume scintillator crystal and to set the basis for the construction of a position sensitive large volume scintillator detector.

The project requires the simulation, production and test of a Position Sensitive prototype which is capable to provide, on an event by event basis, the image produced by the scintillation light on the photocathode. Possible scintillators which can be used in the project are NaI, LYSO, CsI(Tl) and the very promising novel materials $\text{LaBr}_3(\text{Ce})$ and CeBr_3 [1-11].

Almost nothing is known on the imaging properties of position sensitive detectors that use several centimeters thick scintillator crystals and medium-high energy γ rays. In fact, even though gamma imaging is a hot topic in applied physics [12-15], the crystals used in such applications have a front surface of 50-100 cm^2 and thickness of few millimeters only, which reduces the detector efficiency down to zero for medium and high energy γ rays. In addition the surfaces are treated to completely absorb the scintillation light and this significantly worsens the energy resolution of the detectors, as approximately 10% of the scintillation light is collected by the photo-sensors. Figure 1 shows the percentage of photons which arrives on the photocathode in the case of incident 662 keV γ rays which have deposited all the energy in a 3"x3" $\text{LaBr}_3:\text{Ce}$ detector [17]. The value is plotted versus the Z coordinate of the γ -ray first interaction point. The plot in the left panel is relative to a 3"x3" $\text{LaBr}_3:\text{Ce}$ detector with fully absorbing surfaces while the plot in the right panel correspond to a detector with fully diffusive surfaces.

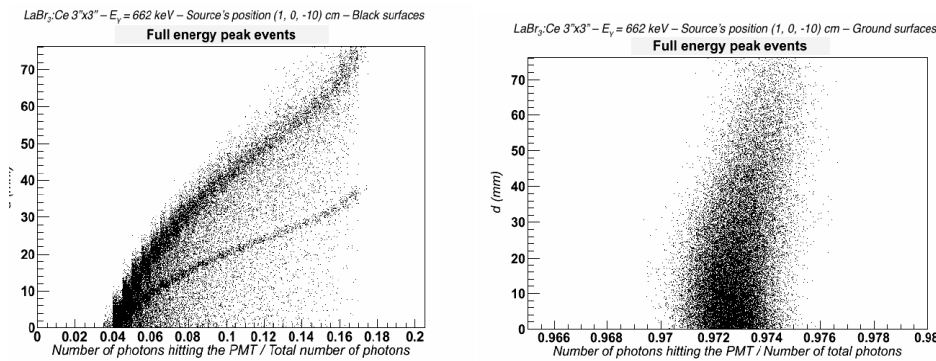


Fig 1: Left panel: the simulated percentage of scintillation photons which arrive at the photocathode in a cylindrical 3"x3" $\text{LaBr}_3:\text{Ce}$ crystal with dark surfaces. Between the crystal and the photocathode a layer of 8 mm glass has been inserted to take into account the crystal encapsulation and the PMT glass window. Right panel: the same plot as in the left panel but, in this case, the crystal has diffusive fully reflecting surfaces. Note the difference in the x axis values. The quantity d represents the distance from the front face ($d=0$) along the Z axis of the detector; $d = 73$ mm corresponds to the end face of the crystal coupled to the PMT through a 8 mm glass window. In the simulation a collimated beam of 662 keV γ rays was used. The γ -ray beam enters into the detector 1 cm away from the center of the crystal front face [17].

The application fields of such kind of devices range from fundamental research to astrophysics, homeland security and medical areas. In nuclear physics basic research and in particular in γ -ray spectroscopy, the efficiency for medium-high energy γ rays and the energy resolution are critical parameters. The imaging properties of a detector are extremely useful to reduce the Doppler Broadening effect in experiments where the γ -ray source moves with relativistic velocity (see figure 2). These beams are, for example, used in the study of nuclei far from the stability line and may reach velocities up to $v/c = 0.6$ and more. In such kind of measurements, the energy of the γ rays emitted by the moving source in the laboratory system (even though monochromatic in the CM system) is Doppler shifted and in the energy spectra the full absorption peak is broadened and degraded because of the size of the detector front face. Such effect becomes larger i) as the v/c of the source increases and ii) as the distance source-detector decreases. The localization of the interaction point of the γ ray inside the crystal (even with a position resolution of 1-2 cm) could reduce or eliminate such effect, recovering the intrinsic performances of the detector. In the case of sources with a low v/c an imaging detector will allow the reduction of the distance from the target increasing, consequently, the total efficiency of the apparatus and the identification of the γ -ray interaction point will allow the reduction of the Doppler Broadening effect.

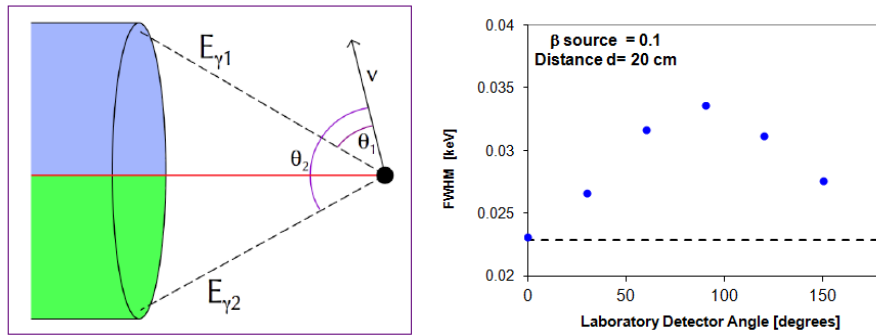


Fig. 2: left panel: a schematic view of the Doppler Broadening effect. The drawing shows a γ -ray source moving with velocity v . The γ rays emitted at angles θ_1 and θ_2 enter and interact in the detector. Even though their energies are identical in the CM system, they are different in the laboratory system. The energy difference $E_{\gamma 2} - E_{\gamma 1}$ is the Doppler Broadening effect. Right Panel: The expected energy resolution for a 3"x3" LaBr₃:Ce detector placed at 20 cm distance from the target at various laboratory angles. Calculations have been performed using a source of monochromatic 1 MeV γ rays moving at $v/c = 0.1$. The straight line indicates the detector intrinsic energy resolution. The Doppler Broadening induced energy resolution at 1 MeV in the CM system for a source moving at $v/c=0.5$ with the detector at 60° is approximately 5 time larger, 180 keV. The error bar for each point is 1 keV. The front-back anisotropy in energy resolution is due to the different energies of the measured γ rays [18].

One important aspect in these kind of measurements is the presence of internal radiation which can be, however, reduced as it is inside the detector and spatially uncorrelated with the γ -ray 'source' which is to be 'identified'. Such kind of background can be rejected i) selecting the γ -ray energy (in this case a good energy resolution is required) or ii) through Pulse Shape Analysis techniques. In the case of LaBr₃:Ce crystals the internal radiation is a strong source of background as (approximately 2 evt/sec/cm³). Such radiation is generated by ¹³⁸La and the decay chain of its heavy homologue ²²⁷Ac. In the case of alpha induced background from the ²²⁷Ac decay chain, as figure 3 evidences, PSA techniques are capable to identify and rejects the alpha induced events [19].

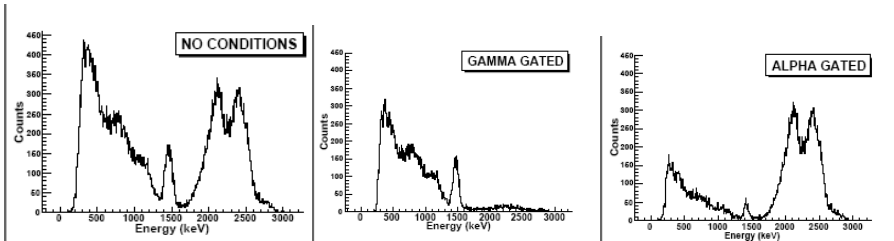


Fig 3 – The internal radioactivity and natural background spectra measured with the $\text{LaBr}_3:\text{Ce}$ detector. The left panel spectrum shows the measurement in single with no condition in the PSA. The middle and right panels show the spectra obtained requiring an alpha or γ -ray signal through Pulse Shape Analysis [19].

An extremely powerful tool to analyze the position sensitivity of large volume scintillator is MonteCarlo simulations. The SCIDRA [ref] and GEANT4 [ref] libraries have been used as a tool to understand the way scintillation photons arrive at the photo-sensors (see for example figure 1). In case of detection of high energy γ rays it is important to stress that the scintillator surfaces must reflect the scintillator light, to maintain the best possible efficiency and spectroscopic performances, although reflections make more difficult to retrace the interaction points (see figure 4).

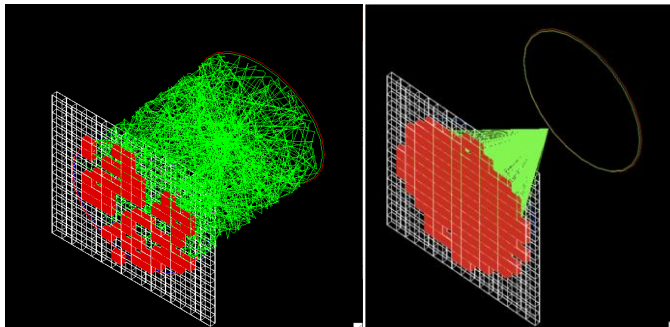


Fig. 4: Left panel: the tracks followed by the photons in the case of fully diffusive surfaces from a simulation with GEANT4. Right Panel: the tracks followed by the photons in the case of perfectly dark surfaces from a simulation with GEANT4 [20].

Within this project several solutions are planned to be tested to verify their performances and the optimal position resolution, photo-sensor technologies and algorithm, namely:

- 1) Cylindrical medium 1''x1'' and large volume 3''x3'' $\text{LaBr}_3:\text{Ce}$ scintillator coupled to position sensitive photomultiplier (PSPMT)
- 2) CsI (of various thicknesses) and Cylindrical large volume 3''x3'' $\text{LaBr}_3:\text{Ce}$ scintillator coupled to an array of Silicon Drift Detectors (SDD)
- 3) Rectangular large volume scintillator with multi-face photon-detection

Cylindrical medium 1"x1" and large volume 3"x3" LaBr₃:Ce scintillator coupled to position sensitive photomultiplier (PSPMT)

In this part of research activity the position sensitivity of one cylindrical small volume (1"x1") and one cylindrical large volume (3" x 3") LaBr₃:Ce crystals have been measured and simulated using collimated beams of 662 keV γ rays.

In the first test, the PMT used was a standard Photonis CLARITY XP5031 with lime glass window. The PMT front window was covered by black tape leaving unshielded only a small region of the photocathode (see figure 5 and 6). The right panel of figure 5 shows how the energy resolution scales with the size of the window. The smaller is the windows the worse is the energy resolution as a reduced number of scintillation photons are measured by the PMT. As expected, using the unshielded PMT a value of 3.5% at 662 keV was found.

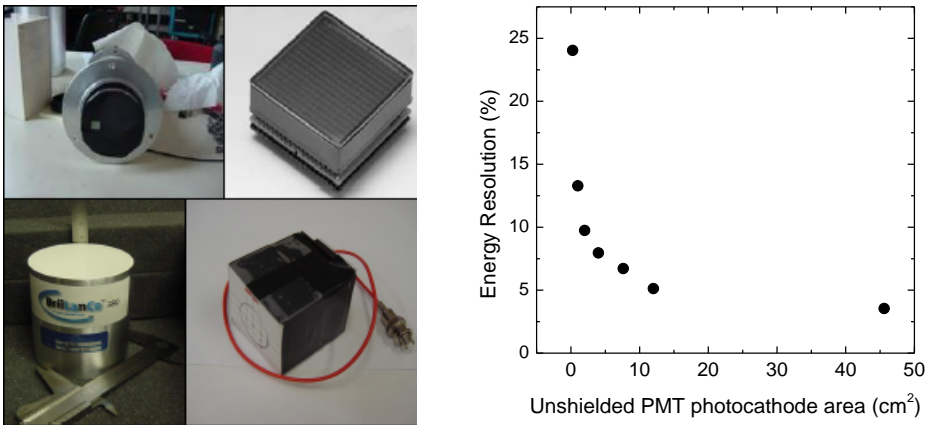


Fig 5: Left panel: a composition of 4 pictures showing the shielded PMT (left upper picture), the PSPMT (right images) and the 3"x3" LaBr₃:Ce crystal. Right panel: the energy resolution at 662 keV measured in a 3"x3" LaBr₃:Ce crystal varying the size of the window on the shielded PMT (the photocathode has a surface of 46 cm²). As expected the energy resolution improves as the open window in the PMT increases in size [17-21].

The position sensitivity using this kind of simple device has been measured using a collimated source of 662 keV γ rays moving along the crystal diameter and changing the position of the unshielded window on the photocathode. The plots in figure 6 show the measured position of the full energy peak, namely the average number of measured photoelectrons. In each plot a picture of the position of the window on the PMT is shown in the upper left part and each of the 5 points correspond to the x coordinate of the collimated 662 keV γ -ray collimated beam. A clear signal of position sensitivity is evident in the plot. In fact γ rays which enter in different positions produce different intensity patterns on the photocathode .

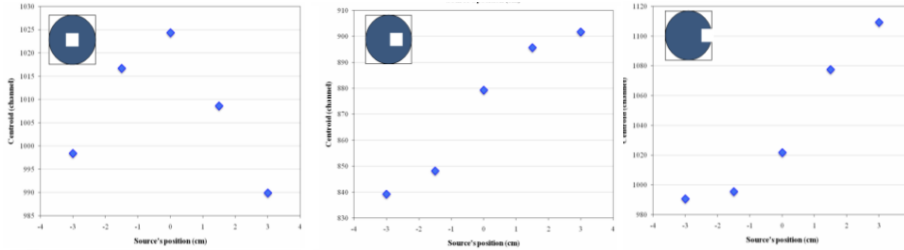


Fig 6: The plots show the measured position of the full energy peak, namely the average number of measured photoelectrons, when 662 keV have been deposited in the detector. In each plot, the position of the window on the PMT is shown in the left upper part and each of the 5 points corresponds to the x coordinate of the collimated γ -ray beam [20-21].

The previous measurements clearly show that, in average, the image produced by the γ rays on the PMT photocathode changes with the γ -ray interaction point [20-21]. In a second phase of the work the LaBr₃:Ce crystal has been coupled to a PSPMT tube (Hamamatsu XP5300-100 Mod8, see the right images of the right panel of figure 5).

As a first step the PSPMT was coupled to a small 1" x 1" LaBr₃:Ce. In this case only 16 (out of 64) segments are coupled to the LaBr₃:Ce detector. The measured average position of the 662 keV full energy peak measured in each segment was plotted relative to the segment x-y coordinates. In figure 7 the measured contour plots are shown: a position sensitivity is evident also in a 1" x 1" detector and a PSPMT.

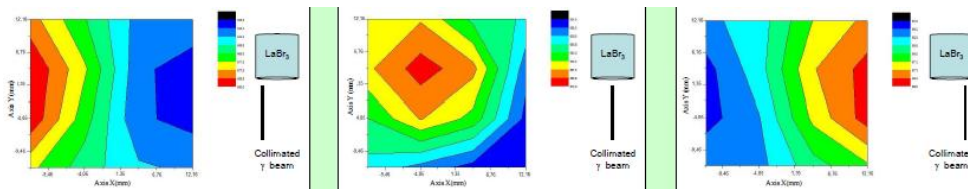


Fig. 7: The plots show the image produced in a 1" x 1" LaBr₃:Ce scintillator with a collimated 662 keV γ -ray beam measured on the segmented anode of a H8500C-100 Mod 8 phototube. In the central plot the collimation pointed approximately at the central position, in the left and right plots the collimated beam of γ rays was at -7 and +7 mm away from the centre. The values on the Z axis represent the position of the centroid of the full 662 keV energy peak [17-22].

The position sensitivity in a 3" x 3" LaBr₃:Ce crystal have been also simulated using the GEANT4 libraries. The size of the detector is large enough to provide good full energy peak efficiency, even in the case of high energy γ rays.

In the simulations, a collimated monochromatic γ -ray beam of energy $E=662$ keV enters into the detector. For each incident γ ray the positions of the interaction points (IP) and the energy there deposited are extracted. Each IP generates a flash of scintillation light which, photon by photon, is followed up to its absorption or detection by a photosensor. In this way it is possible to simulate the spectra measured in both the shielded PMT and in the PSPMT. Figure 8 compares the measured results already shown in figure 6 with the simulations of the same system [20,23]. Measurements

and simulations produce very similar curves. The error bars do not have any statistical origin but indicate the size of the PMT window.

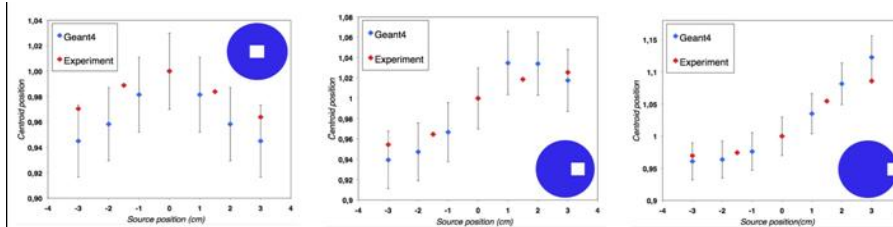
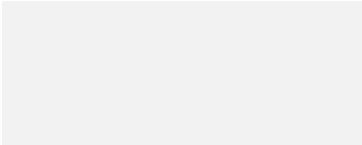


Fig. 8: the comparison between the measurements of fig. 6 and the simulated (using GEANT4) results. In particular in the plots the measured and calculated relative position of the full energy peak (the average number of photoelectrons) for different positions of the collimated beam and PMT window is shown. The energy of the used γ rays is 662 keV. In each plot the position of the window on the PMT is shown in the upper left part and the 5 points correspond to different x coordinate of the collimated 662 keV γ -ray beam [20,23].

A more detailed example of the results of GEANT4 simulations for a 3''x3'' LaBr₃:Ce crystal is shown in figure 9. Two different detector configurations have been simulated : in the left panel a detector with dark surfaces and in the right panel a detector with diffusive surfaces are assumed. The graphs show all the processes of the simulation for six selected events, from the energy deposited by the incident γ rays up to the image produced on a segmented photocathode.

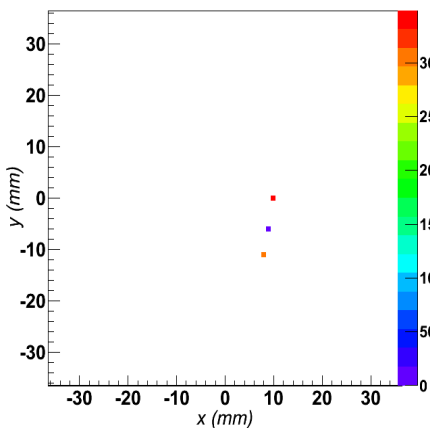
it is evident from the plots that dark surfaces provide in average the best imaging performances on an event by event basis but, as 90% of the scintillation photons are lost, scarce energy resolution. In the case of diffusive surfaces, the depth of interaction of the incident γ -ray is critical, namely the distance between the γ -ray interaction point and the photocathode [20,23]. In general, if a γ ray interacts in the second half of the detector depth, the position sensitivity on an event by event basis is evident. In case of interaction in the first half, the position sensitivity can be recovered on an event by event basis only using algorithms.



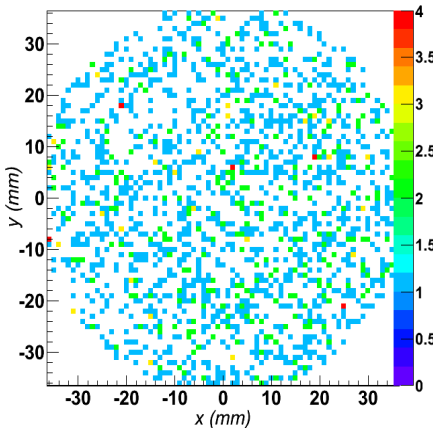
3''x3'' – 662 keV – Source position (1, 0, -10) cm – DARK SURFACES

d = 0 - 5 mm

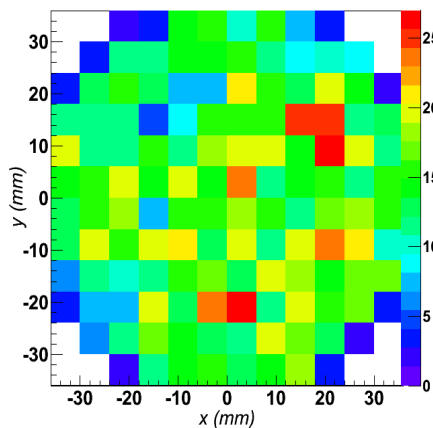
Energy deposition



Photocatode image

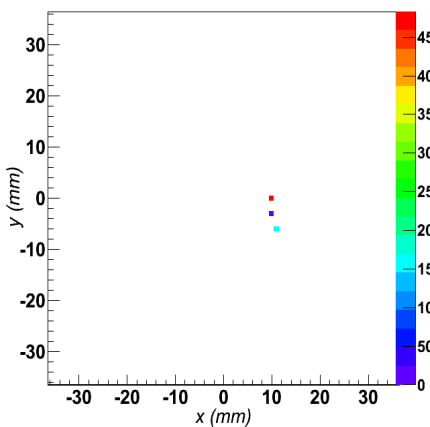


PMT image

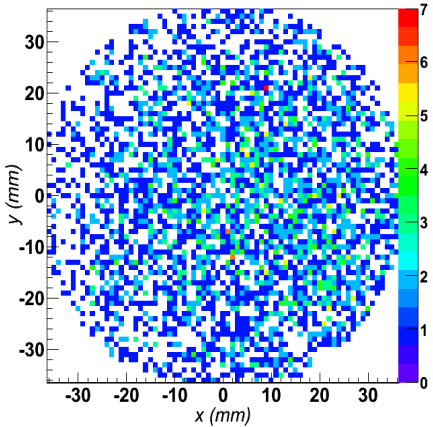


d = 40 - 45 mm

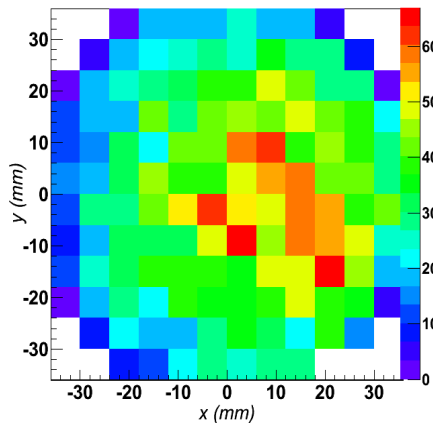
Energy deposition



Photocatode image

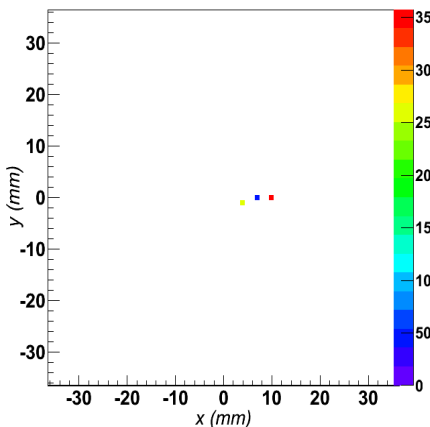


PMT image

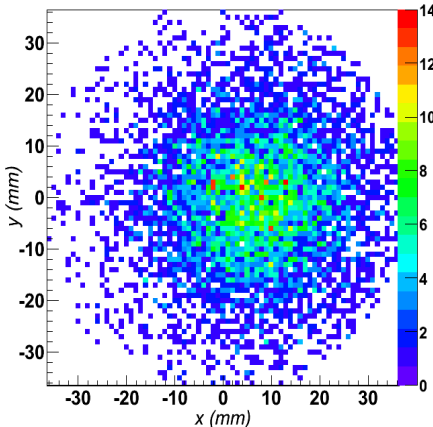


d = 60 - 65 mm

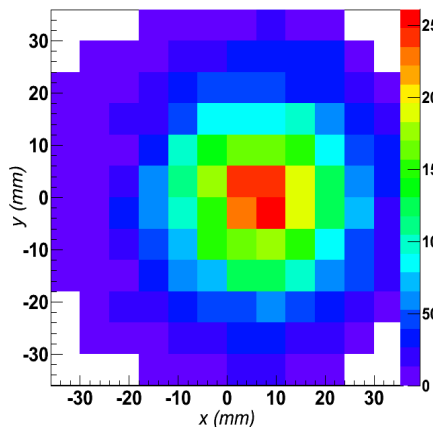
Energy deposition

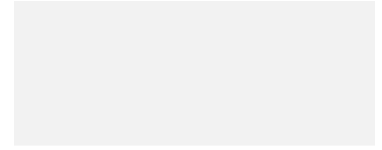


Photocatode image



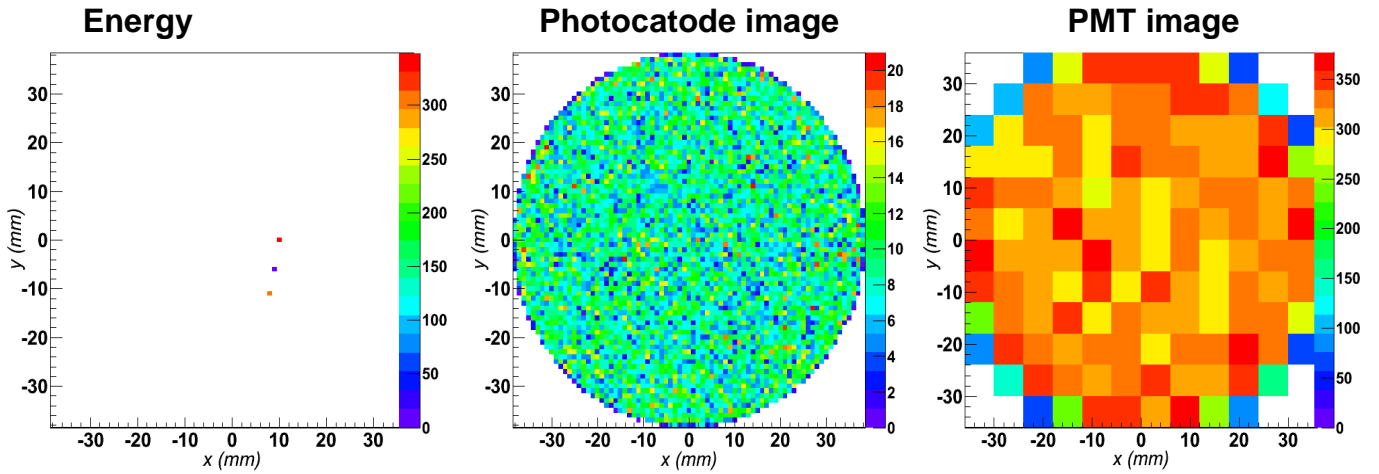
PMT image



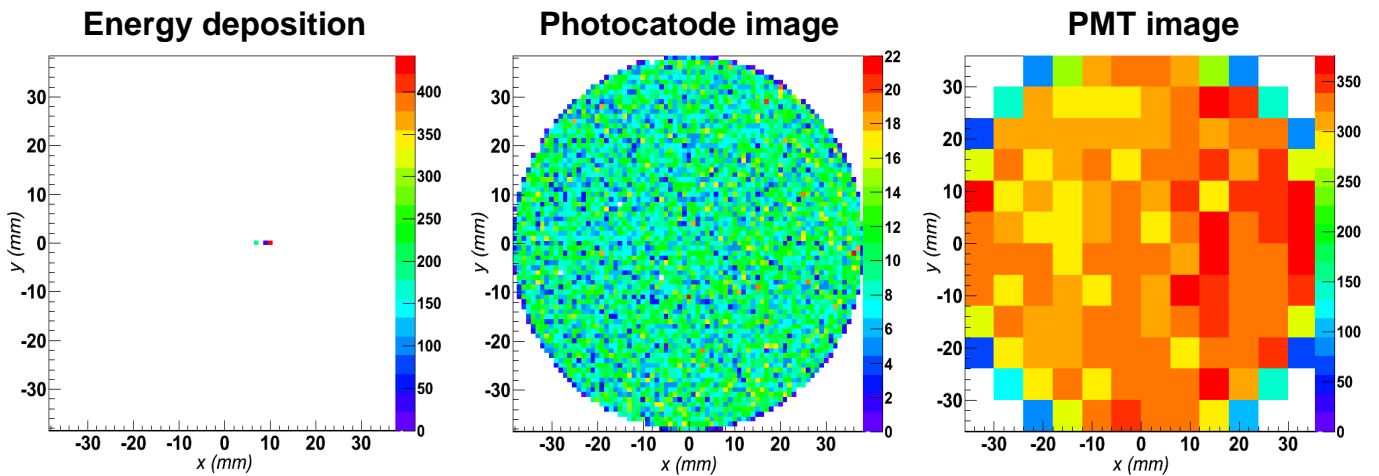


3"x3" – 662 keV – Source position (1, 0, -10) cm – FULLY DIFFUSIVE SURFACES

d = 0 - 5 mm



d = 40 - 45 mm



d = 60 - 65 mm

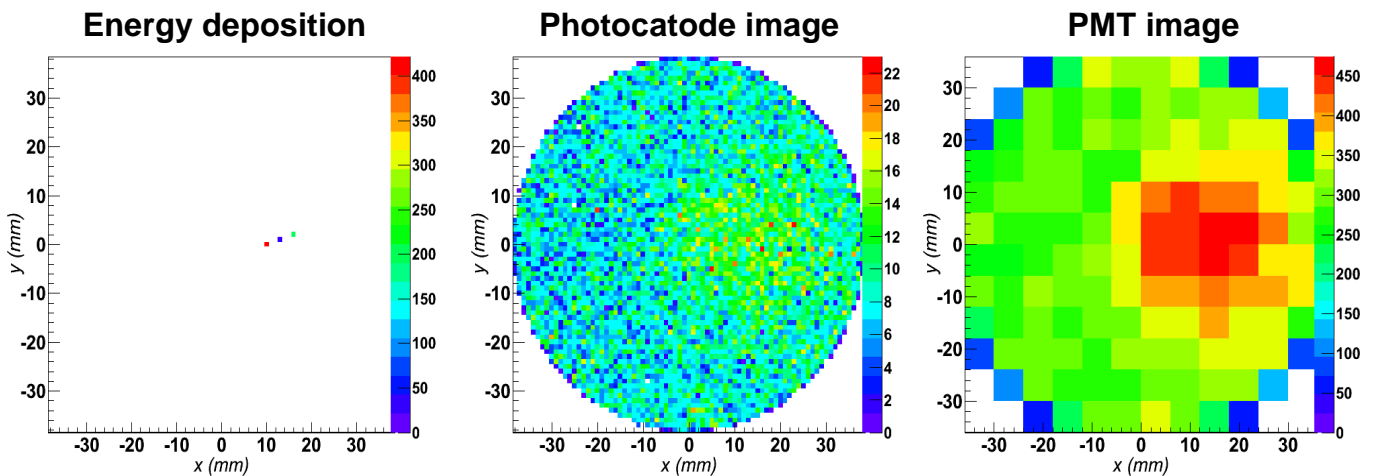


Fig. 9: The plots show the position in the x-y axis of i) the energy deposition (first column), ii) the light sensor (middle column) and iii) the segment (right column) hit position of the scintillation photons for a typical γ -ray event which deposit 662 keV. The plots shows that in the crystal with dark surfaces (left panel) the position sensitivity is much better than in the fully diffusive crystal (right panel). It is also evident that the sensitivity improves as the hit position approaches the light-sensor [20,23].

CsI (of various thicknesses) and Cylindrical large volume 3"x3" LaBr₃:Ce scintillator coupled to an array of Silicon Drift Detectors (SDD)

In this second approach the work has been done in collaboration with the "Politecnico di Milano" and Prof. C.Fiorini [24-26]. This approach uses the innovative solution of SDD as a photo-sensor coupled to a 5 cm x 5cm CsI scintillator block with thickness of 1,2 cm. Measurements with a 5 cm thick CsI scintillator and with a LaBr₃:Ce scintillator are also foreseen in the near future.

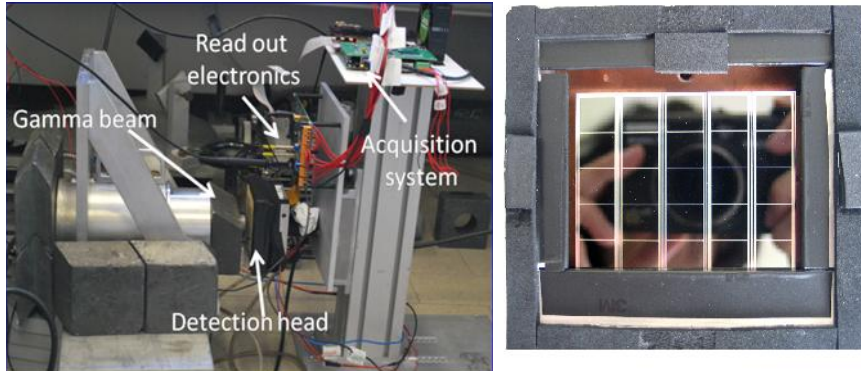


Fig. 10: left panel: a picture of the experimental setup used for the measurement of position sensitivity with CsI and Silicon Drift Detector (SDD) [24]. Right panel: a picture of the SDD matrix used in the measurements.

The picture in figure 10 shows the experimental setup used for the measurements. The collimated 662 γ -ray source (the same used for the measurement discussed in the previous sections) is on the left. The detector is in the middle of the picture while the holder and the electronics are on the right part. The measurements have been performed using a cylindrical collimator of 1 mm diameter hole and using different algorithms. The left panel of figure 11 shows the results of the analysis for a 60x50x10 mm CsI detector. The 8 spots visible in the figure correspond to the superposition of 8 measurements. In each measurement the γ -ray beam was shifted 5 mm and the FWHM of each spot was ~ 2.5 mm. The right panel of figure 11 is equivalent to the left panel but using a 20 mm thick detector. The width of each spot, also in this case, was ~ 2.5 mm.

A new measurement campaign is foreseen in 2013 using a 5 cm thick CsI and a 3"x3" LaBr₃:Ce scintillators.

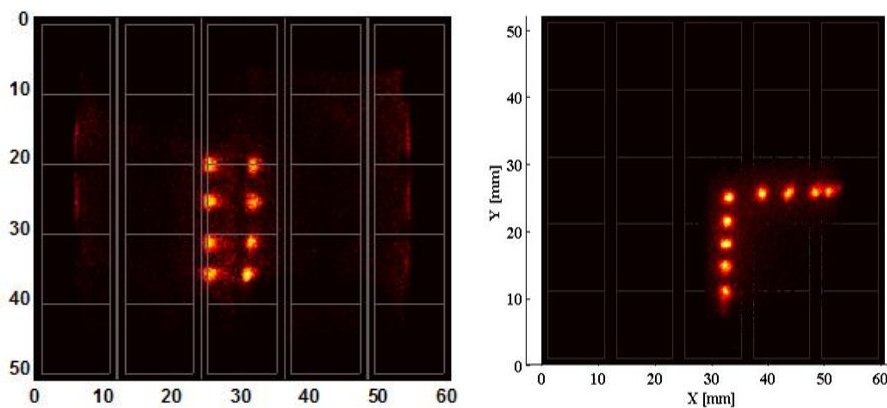


Fig. 11: The results of the position sensitivity measurements achieved using a 10 mm (left panel) or a 20 mm (right panel) thick CsI crystal coupled to an array of Silicon Drift Detectors. [24].

Rectangular large volume scintillator with multi-face photon-detection

The principal idea of this approach is to cover several faces of a cuboid scintillator crystal with position sensitive photo-sensors in order to determine the interaction points of penetrating γ rays in 3D. This solution provides the best possible position resolution for the initial interaction point, as required for Doppler correction of γ -ray energies in nuclear structure experiments with fast moving emitters. In addition, tracking of the path of γ rays through the scintillator may be possible. Thereby events with more than one γ ray entering a scintillator crystal at the same time can be identified and either discarded or even corrected, resulting in improved spectrum quality in experiments where high γ -multiplicities occur. γ -ray tracking provides also the possibility of gamma imaging, exploiting the Compton camera principle.

Within this project a 3D position-sensitive scintillation detector is planned to be developed, which will serve as part of a hybrid detection system composed of a position-sensitive scintillation front-detector and a conventional Ge back-detector. This hybrid-detector is intended to be used for in-beam spectroscopy of exotic atomic nuclei produced by fragmentation reactions at relativistic beam energies. The main characteristics of the hybrid-detector are an intrinsic energy resolution of 1-2% in the interesting energy range from 300 keV to 3 MeV and a position resolution of about 3 mm for the first interaction point in the scintillator. For typical velocities of the gamma emitting nuclei of $v/c = 0.4 - 0.6$ and source-to-detector distances of 10 cm to 15 cm, as previously discussed, the energy resolution after Doppler correction is dominated by the intrinsic resolution of the system.

Simulation showed that a scintillator thickness of 15 mm yields the largest efficiency when coupled to a Ge detector with at least 70 mm thickness. Using LaBr₃ as scintillator detector revealed an energy resolution of about 1 % at 1 MeV gamma energy when adding the contributions of both detectors event-by-event. The intrinsic efficiency for full energy absorption requiring the first interaction in the scintillator and the subsequent interactions in the Ge crystal is about a factor 4 to 5 lower than the efficiency of a large volume Ge detector of the size of a EUROBALL crystal without front scintillator. However, for the intended application EUROBALL detectors would need to be placed at least 70 cm away from the source to limit their solid angle in order to maintain 1-2 % energy resolution. Thus the hybrid system covering 20-30 times larger detection solid angle per hybrid-detector unit provides a factor five larger total full energy efficiency despite the lower intrinsic efficiency.

The close proximity to the gamma source leads to considerable parallax effects in a 15 mm thick front-detector. Therefore 3D position sensitivity is mandatory to achieve 3 mm position resolution of the first interaction point.

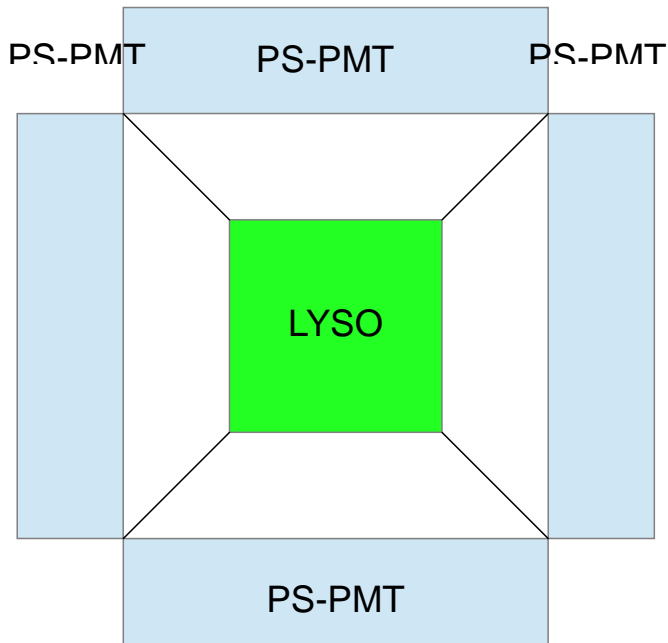


Fig. 12: Schematic layout of the LYSO Cube-Detector system.

To investigate the potential of the multi-face photon-detection a test system has been built, using a $34 \times 34 \times 34 \text{ mm}^3$ LYSO crystal coupled to position-sensitive PMTs (Hamamtsu 8500 series). Truncated square plastic pyramids served as light guides between crystal and PMT as shown schematically in fig. 12. The centroid of the light distribution on each side was obtained employing a conventional resistive chain network on each PMT. The obtained centroids and the relative light intensity provide a measure of the interaction position in 3D. LYSO like $\text{LaBr}_3:\text{Ce}$ has the drawback of severe self-activity. To effectively suppress this self-activity a ^{22}Na source coupled to a reference gamma detector was employed for all investigations. Demanding one 511 keV γ ray to be detected in the reference detector in coincidence with the signals of the cube detector allowed to study the pure response of the other 511 keV γ ray in the cube. Absorption in the PMT material was negligible.

The PMT amplitude signals were first calibrated by uniformly illuminating the crystal with the ^{22}Na source. Then the source was collimated using a Pb block with a 2 mm hole. Fig. 13 shows the projection of the light distribution obtained for three different hole positions, being about 7 mm apart from each other. The intensity drop from left to right corresponds to the attenuation of the 511 keV γ rays in the depth of the crystal. A sum energy of 511 keV was demanded in the analysis for both the cube-detector and the reference detector.

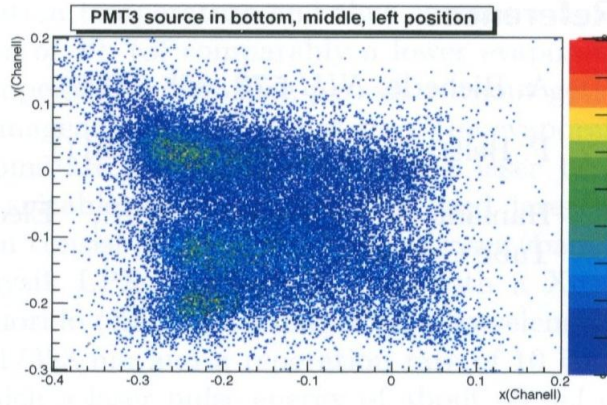


Fig. 13: Relative x,y distribution for three different y positions of the source situated at the left side of the cube.

Employing all channel information enables the reconstruction of the interaction points in 3D as shown in fig. 14. Already in the test runs a 3D position resolution of 3-4 mm FWHM has been achieved. Next steps will be to optimize the position determination by individual anode readout of the PMTs. It has been shown previously [28] that this can significantly improve the light centroid measurement because the strong gain differences of the anodes can be corrected for. At the same time the optimal pixel number will be determined in order to reduce the number of electronics channels to the needed minimum.

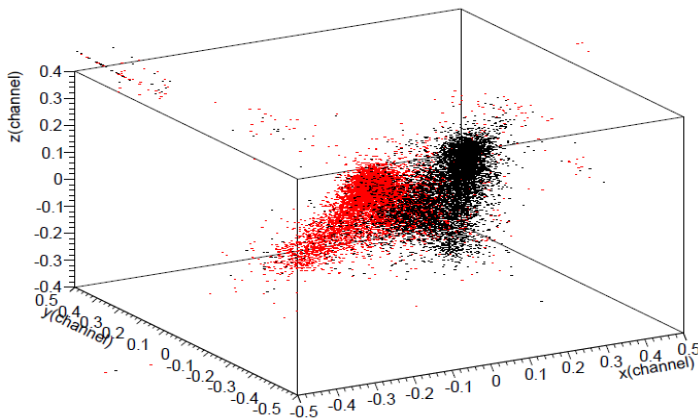


Fig14: 3D position reconstruction for two different source positions being 7 mm apart from each other.

Position Sensitivity in novel Hybrid semiconductor-scintillator detector

The investigations of light response for gamma rays performed in Kraków in relation to the PARIS project comprised simulations of light propagation in detectors of different sizes.

Using GEANT4 Monte Carlo software the propagation of light produced by gamma rays in scintillation detectors have been simulated for two detectors: cubic LaBr_3 crystal ($2'' \times 2'' \times 2''$) and PARIS phoswich detector LaBr_3 ($2'' \times 2'' \times 2''$) / NaI ($2'' \times 2'' \times 6''$). The light responses for the 1 MeV gamma rays emitted into the center of the crystal or into the left side position have been calculated for each detector.

The obtained light response of cubic LaBr_3 crystal ($2'' \times 2'' \times 2''$) for 1 MeV gamma rays presented in Fig. 15 shows the possibility of the interaction point discrimination by the light output. The differences visible on Figure 15 (left and right panel) indicate the possibility of obtaining precise gamma energy deposit information by usage of segmented photodetector.

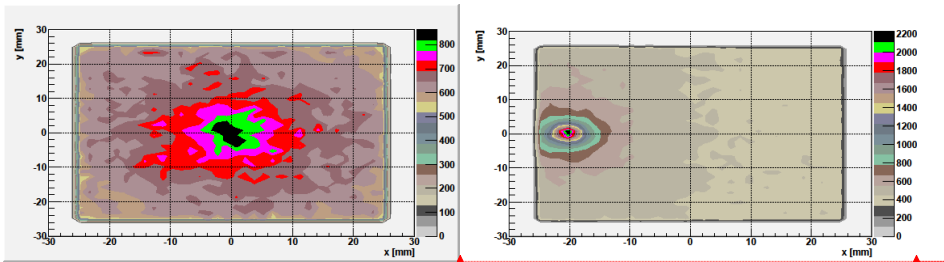


Figure 15. Distribution of scintillation light measured on back side of cubic $2'' \times 2'' \times 2''$ LaBr_3 crystal. Scintillation light was produced by absorption of 1 MeV gamma ray, which was emitted: left panel - into the center of the LaBr_3 , right panel - into left side of the crystal (point $x, y = [-2 \text{ cm}, 0]$).

In the case of response for 1 MeV gamma rays of phoswich detector, composed of $2'' \times 2'' \times 2''$ LaBr_3 connected to $2'' \times 2'' \times 6''$ NaI , simulation results show no dependence on the interaction point. Obtained results presented in Fig. 16 for this detector are very similar for different irradiation (into the center and to the side). They indicate that there is no possibility to get information of the energy deposit positions by measuring the scintillation light distribution.

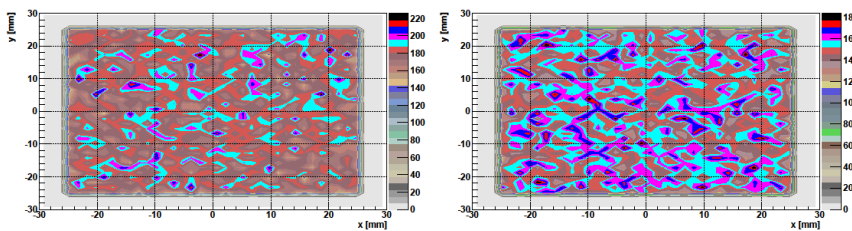


Figure 16. Distribution of scintillation light measured on back side of phoswich detector ($2'' \times 2'' \times 2''$ LaBr_3 + $2'' \times 2'' \times 6''$ NaI). Scintillation light was produced by absorption of 1 MeV gamma ray, which was emitted: left panel - into the center of the LaBr_3 , right panel - into left side (point $x, y = [-2 \text{ cm}, 0]$).

Obtaining information on energy deposit position by the light measurement depends mainly on length of detector and is not possible for longer phoswich detector (LaBr₃+NaI). Due to longer path of light from the gamma interaction point to the photodetector information on interaction point is lost.

Summary Table:

	Italy	Germany	Poland
Money used in 2012	0	0	
People	Simone Ceruti (Student) 2 weeks, Stefano Lodetti (student) 2 weeks, Agnese Giaz (student) 4 weeks Franco Camera (4 weeks) Nives Blasi (2 weeks) Sergio Brambilla (2 weeks)	Tugba Arici (master student) full time, Ivan Kojouharov 4 weeks, Frederic Ameil 4 weeks, Edana Merchan 4 weeks and Simone Ceruti 6 weeks working on the project	
Activity	See text	See text	
Publications	One in preparation	no	
Talks	2 Talks in Bormio 1 Talk in Varenna conferences		

- [1] C.M.Rosza et al available at www.detectors.saint-gobain.com
- [2] A.Iltis et al. NIM A563(2006) 359
- [3] M.Moszynski et al. NIM A567 (2006) 31
- [4] M.Moszynski et al. NIM A568 (2006)739
- [5] W.Mengesha et al. IEEE TNS NS-45(1998)456
- [6] P.Menge et al. NIM A579(2007)6
- [7] R. Nicolini et al NIM A 582 (2007) 554–561
- [8] A.Giaz et al to be submitted on NIM A
- [9] K.S. Shah et al. IEEE TNS NS-52 (2005) 3157
- [10] A. Maj et al ACTA PHYSICA POLONICA B40 (2009)565-575
- [11] W.M. Higgins et al. J. Crys. Growth 310 (2008) 2085
- [12] J.W.Scrimger, R. G. Baker, Phys. Med. Biol. 12 (1967) 101
- [13] R.Pani et al. NIM A571 (2007) 187 and R.Pani et al. IEEE NSS-CR (2008) 1763
- [14] R.Pani et al. NIM A576 (2007) 15
- [15] D.R. Kuhn et al. IEEE TNS 51 (2004) 2550
- [16] M.N.Cinti et al. IEEE NSS-CR (2008)
- [17]] F. Birocchi, N. Blasi, F. Camera et al 2010 IEEE Nuclear Science Symposium and Medical Imaging Conference (2010 NSS/MIC) Pages: 198-200 DOI: 10.1109/NSSMIC.2010.5873746
- [18] F. Camera et al Private Communications
- [19] F.C.L. Crespi et al. NIM A602(2009)520-524
- [20] F. Birocchi, N. Blasi, F. Camera et al. 2009 IEEE Nuclear Science Symposium and Medical Imaging Conference (NSS/MIC 2009) Pages: 1403-5 DOI: 10.1109/NSSMIC.2009.5402329
- [21] Federica Coniglio, Tesi di laurea Triennale, Dipartimento di Fisica dell'Università di Milano via Celoria 16, 20133 Milano.
- [22] Riccardo Avigo, Tesi di laurea Triennale, Dipartimento di Fisica dell'Università di Milano via Celoria 16, 20133 Milano.

- [23] Francesca Birocchi, Tesi di laurea Magistrale, Dipartimento di Fisica dell'Università di Milano via Celoria 16, 20133 Milano.
- [24] C.Fiorini et al. IEEE TNS 53 (2006) 2392
- [25] C.Fiorini et al. NIM A573 (2007) 84
- [26] C.Fiorini et al. IEEE NSS-CR (2008) 3961
- [27] Paolo Busca, PHD tesi, Politecnico di Milano, Piazza leonardo da Vinci, Milano
- [28] C. Domingo-Pardo, N. Goel, T. Engert, J. Gerl, M. Isaka, I. Kojouharov, H. Schaffner, IEEE Trans. Med. Imaging, 12 (2009) 2007

Working package 5:

Test with gammas of a LaBr₃+LaCl₃ truncated pyramid

Montecarlo simulations with R3BRoot were performed to calculate peak and peak to total efficiencies with protons see <http://161.111.23.177/r3bmeeting/>.

Very interesting results were obtained using the module MPD4 of Mesytec (4 channel pulse shape discriminator module) that allows to separate the LaBr signals of gamma radiation from the LaCl ones. Though this module is used to separate neutrons from protons, we will use to separate different fast gamma signals coming from the phoswich crystals.

⁶⁰Co and ²³Na were used for this test of gamma radiation. In this case the phoswich pyramid was used and a preamplifier was connected to the Si PM. The PM was supplied with 1000 V by a high voltage power supply and the amplifier to the module MPD4. This module allowed us to separate in time the signal of LaBr and LaCl using the proper gate time.

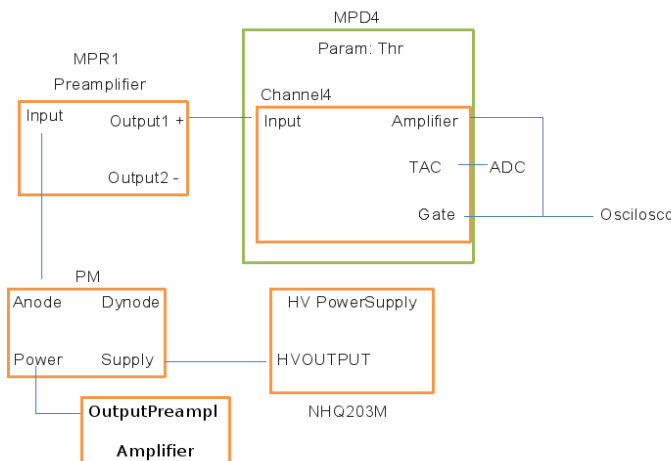


Fig 21: Electronic experimental setup for the test of the separation of gamma radiation LaBr and

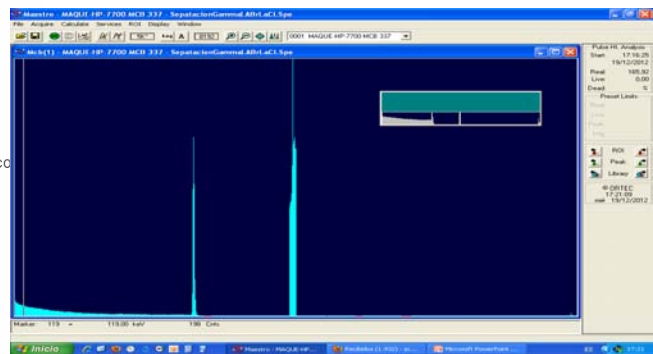


Fig 22: LaBr₃ (right) gamma radiation signal separated of LaCl₃ (left) one with the phoswich pyramid crystal

Two different sources have been used to determine the gamma efficiency for different energy sources (⁶⁰Co, ²⁷Cs and ²⁶Na). The experimental set-up was the same as the previous commented: A preamplifier (MPR1), an amplifier (ORTEC 671), a SiPM and a high energy power supply (NHQ 203M) to supply with 1000 V the PM. The signal is unipolar and an ADC 926 ADCAM ORTEC MCB is used. The background spectra have been studied and the 3 alphas and gamma peaks from the ²²⁷Ac chain can be seen at the same time. These are the spectra obtained

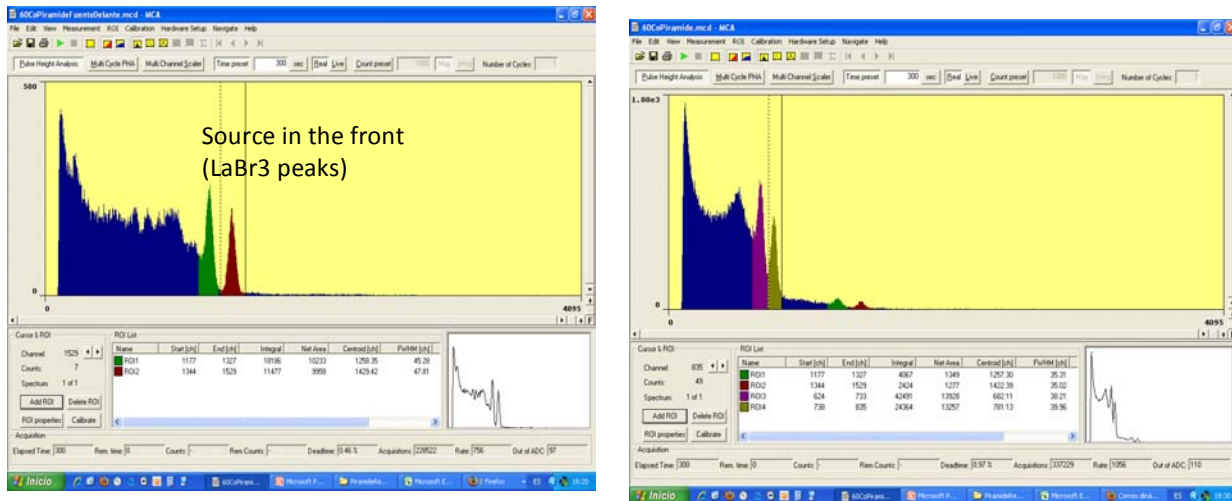


Fig 31: Energy spectra for a gamma radiation of a ^{60}Co source onto the phoswich pyramide crystal. Two different positions of the source: in front LaBr side of the Phoswich to the left, in front of the LaCl side of the Phoswich to the right.

The experimental resolution of the pyramid is presented in the following figure:

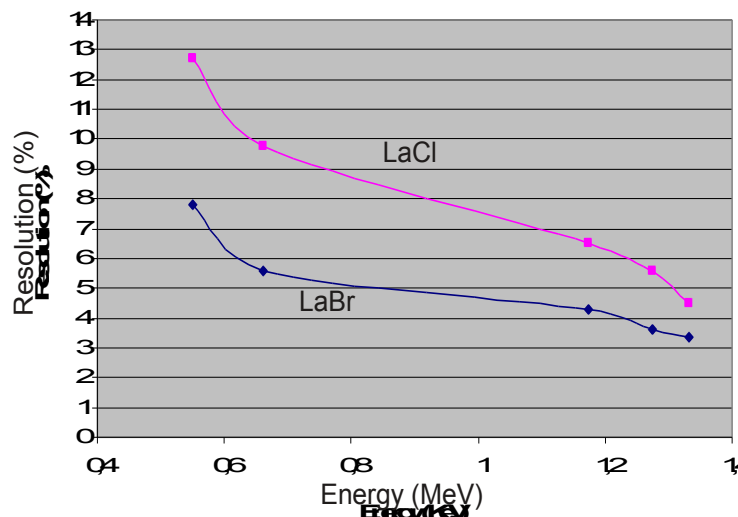


Fig 32: Energy spectra for a gamma radiation of a ^{23}Na source with the phoswich pyramide crystal and for different positions of the source in the crystal

The same experimental test was performed with each of the PMs adapted to the 4 phoswich crystals of CEPA. The results allowed us to calculate the resolution of CEPA. The shaping time used was of 2 us and the gain of the amplifier. Data were measured in April and in October and the resolutions measured in October are 4% higher than in April. However these measurements have to be repeated three or four times more if these changes of the spectra in time want to be seriously considered (It is possible that the optical contact between PM and crystals is not so good as in April).

The gamma radiation and protons efficiency for CEPA has been simulated with R3BRoot, the same as the experimental resolution. We compare in the Figure 35 efficiencies of CEPA for 10 cm (4+6 cm) and when the crystals are 2 cm longer (4+8 cm).

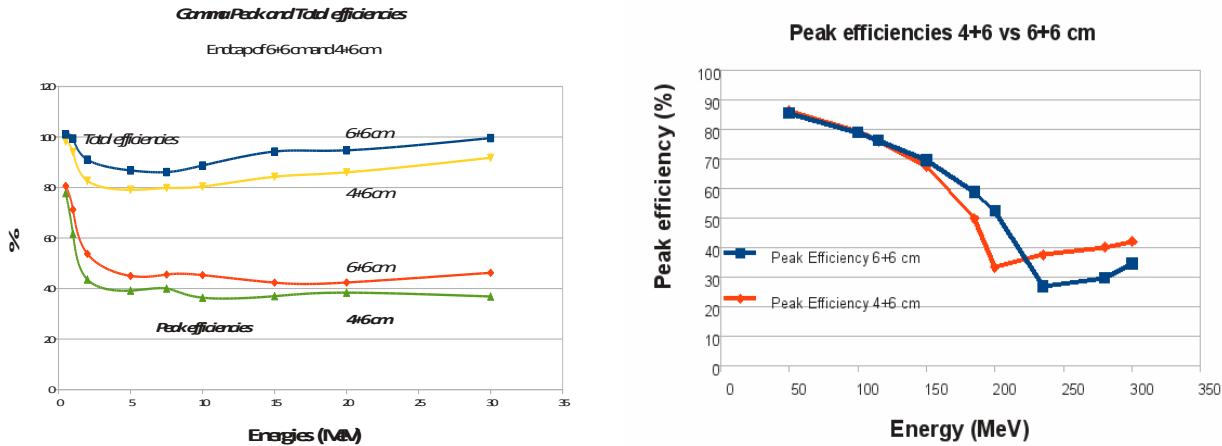


Fig 35: Efficiency simulated with R3BRoot for gamma radiation and protons of whole CEPA (array 4x4)

We have simulated as well the efficiencies for proton and gamma radiation with and without intrinsic crystals resolutions which are dependent on the energy. There is a n increasement when they are included.

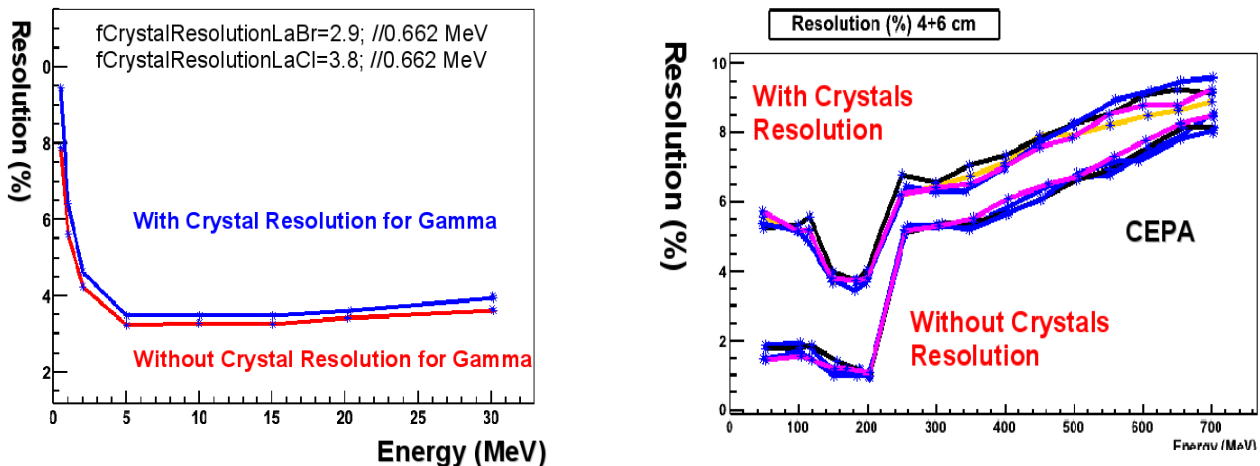


Fig 36: Resolution simulated with R3BRoot for gamma radiation and protons of whole CEPA (array 4x4)

Tests of LaBr₃-NaI phoswich detector with high energy gamma-rays

M. Ziębliński^a, M. Ciemała^a, M. Jastrzab^a, S. Brambilla^d, P. Bednarczyk^a, A. Maj^a, M. Kmiecik^a, M. Dudelo^b, K. Hadyńska-Klęk^{b,c}, P. Napiorkowski^b, B. Genolini^e, Ch. Schmitt^f, N. Yavuzkanat^g

^aIFJ PAN, Kraków, Poland; ^bHeavy Ion Laboratory, University of Warsaw, Poland;
^cUniversity of Warsaw, Poland; ^dINFN Sez. di Milano, Italy; ^eIPN Orsay, France;
^fGANIL, Caen, France, ^gUniversity of York, York, United Kingdom

The response of the phoswich detectors to high energy gamma rays was studied. The set-up, consisting of 3 phoswiches and a single LaBr₃:Ce detector, was exposed to 6.129 MeV gammas from a ²⁴⁴Cm - ¹³C source, and 10.763 MeV photons emitted in the ²⁷Al(p,⁺)²⁸Si reaction. The in-beam measurement was conducted with a 992 keV proton beam from the Kraków Van de Graff accelerator.

We used the discrimination method provided by an Advanced Pulse Stretcher (APS) module developed in Milano [1]. The APS module supplies two Gaussian signals: "fast" proportional to the amplitude of the rapid signal component only (LaBr₃:Ce), and "slow" which is proportional to the energy of the entire signal (LaBr₃:Ce and NaI:Tl). Both of the signals were fed to the multichannel CAEN V785 ADC, as shown in the diagram of Fig. 3. The resulting spectra were acquired in the Kmax environment [2]. During the in-beam test, a fast active splitter was used to duplicate the PMT signal which was digitized at different frequencies, by the CAEN V1729 (12 bits, 1 GS/s), and the Acqiris DC252 (10 bits, 4 GS/s) digitizers. An example of 2D analysis is shown in Fig. 1.

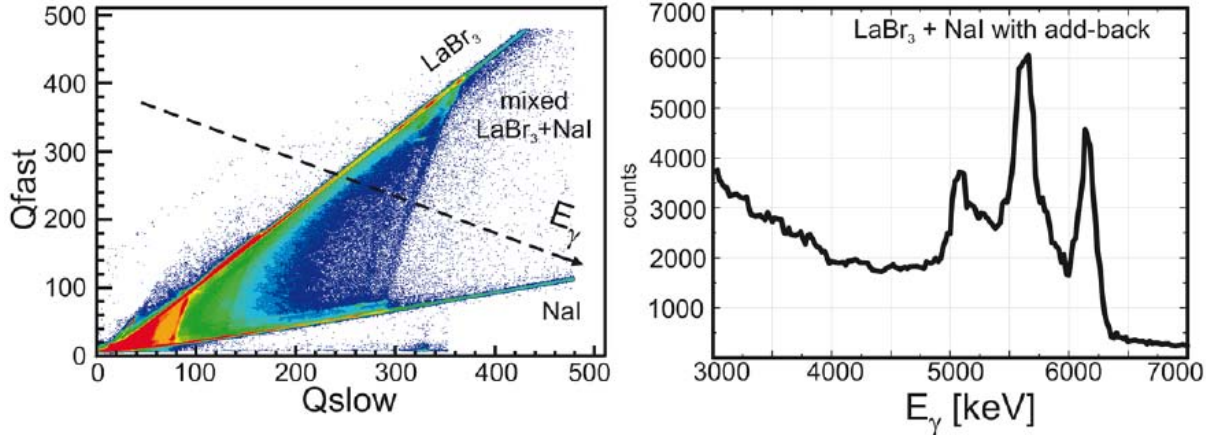


Fig.1. Left: The charges collected in fast and slow gates of phoswich detector measuring 6.13 MeV gamma-rays. Right: The obtained add-back γ -spectrum.

The 2D plot of "Qfast" vs. "Qslow" amplitudes, registered with the APS module, shows a clear separation between the LaBr₃:Ce and NaI:Tl components. The two semi diagonal stripes contain events corresponding to the energy release in the LaBr₃ crystal or in the NaI crystal only. Located between these stripes are events in which the energy deposition was shared between two scintillators. As both crystals had different energy gains, in order to obtain the total energy spectra, we defined a tilted axis that corresponds to gain matched gamma energies (indicated as a dashed line in Fig. 1 left). A projection of the matrix points on this axis provides the full add-back spectrum (see Fig. 1 right). The

signals from PMT were collected. Typical PMT signals, corresponding to $\text{LaBr}_3:\text{Ce}$ and NaI:Tl for 6.13 MeV full absorption peaks, selected by two-dimensional conditions on the "Qfast"- "Qslow" matrix, are presented in Figs. 2a and 2b. An exponential fit provided decay times τ describing the waveforms of reference. These parameters were observed to be valid also for signals induced by photons of $E = 1.3$ MeV and $E = 10.76$ MeV. In Fig. 2c an example of a complex signal produced by a 6.13 MeV photon interacting in both parts of the phoswich is shown.

It turned out that a multi-component fit of the signal amplitudes (at fixed decay times deduced from the signals of reference) accurately reproduced the registered waveforms. The γ -ray energy spectra corresponding to the LaBr_3 -like, NaI -like, and mixed events are shown along with the representative phoswich signals. One can see that in the spectrum of scattered photons (Fig. 2c) the double escape peak is significantly reduced, what illustrates an increase of efficiency of the phoswich with respect to the individual scintillators.

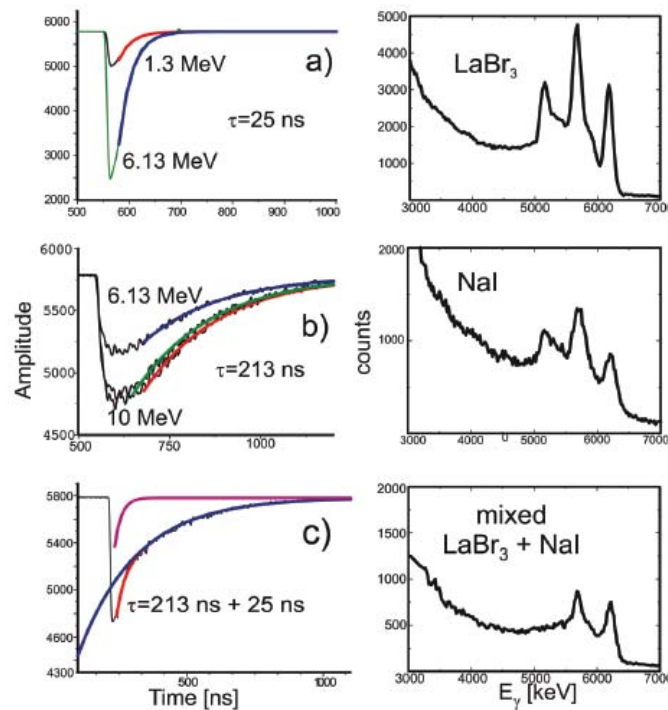


Fig.2. Signals from PMT corresponding to different regions of Qfast-Qslow matrix and gamma spectra reconstructed by charge integration of the filtered detector pulses.

[1] C. Boiano et al., IEEE Transaction on Nuclear Science, 53, 444 (2006).

[2] S. Brambilla et al., Sparrow Corporation Data Acquisition Conference and Workshop , 22-24 March 2005, Daytona Beach, FL (2005).